Semiconductor Physics, Quantum Electronics & Optoelectronics. 2000. V. 3, N 1. P. 45-51.

PACS 68.65, 81.05. E, 81.15. L

AFM study of micromorphology and microscopic growth mechanisms of Hg_{1-x} Cd_xTe LPE epitaxial layers

G.V. Beketov, L.V. Rashkovetskiy, O.V. Rengevych, G.I. Zhovnir
Institute of Semiconductor Physics, NAS of Ukraine,
45, Prospect Nauki, 03028, Kyiv, Ukraine

Abstract. Mercury cadmium telluride epitaxial layers exhibiting large areas with nearly atomically-flat surface were grown using liquid phase epitaxy (LPE) from Te-rich solution in closed system. Evolution of surface morphology during different steps of LPE growth was studied using scanning probe microscopy. Various growth features including monomolecular steps were observed. Both scanning probe microscopy (SPM) images and surface composition analysis with X-ray fluorescence spectroscopy clearly showed that vapor phase growth at the melt homogenization step contributed to epilayer formation and further evolution of its morphology.
It was found that formation of flat areas proceeds via a dislocation-controlled monomolecular step growth mechanism. Phenomenological estimation of local supersaturation conditions giving rise to these areas was given on the basis of the interstep distance of the growth spirals originating from screw dislocations. The results obtained suggest the way of radical morphological improvement of the LPE-grown epilayers.

Keywords: liquid phase epitaxy, scanning probe microscopy, surface morphology.

Paper received 30.12.99; revised manuscript received 04.01.00; accepted for publication 06.01.00.

1. Introduction

Mercury cadmium telluride quasibinary solid solution $Hg_{1-x}Cd_xTe$ still remains a material number one in infrared detector applications. But while sophisticated focal plane arrays (FPA) of sizes as large as 256×256 and more are now well into a manufacturing phase, there remain many unanswered questions about the nature of $Hg_{1-x}Cd_xTe$ alloys, questions, resolution of which would improve the performance, yield and stability of FPAs. Present day IR imaging systems are implemented in the form of n^+p HgCdTe photovoltaic detectors arranged as a 2-D matrix bonded in a hybrid form to a Si chip where signal processing is performed. The current photovoltaic HgCdTe detector technology is based on ion-implanted n^+ junctions on p-type epilayer 10–20 μm thick grown on a lattice-matched substrates transparent for IR radiation within the spectral range of device sensitivity. That is why the epitaxial layer quality is of crucial importance for FPA performances. Three most common epitaxial techniques used for CdHgTe thin film growth are liquid phase epitaxy (LPE), metal-organic vapor phase epitaxy (MOVPE) and molecular beam epitaxy (MBE). Their comparative advantages and disadvantages are summarized in Table 1. Because of the relative cost efficiency combined with high electrical properties LPE has received considerable attention, especially for industrial scale applications. LPE layers are usually grown on <111>B (i.e. Te-terminated) lattice-matched $Cd_yZn_{1-y}Te$ sub-strates from a Te-rich melt. Films produced by LPE can have dislocation densities that reflect the defect densities in the substrate and are free of substructure, due to a dispersion of the threading dislocations through the graded substrate-LPE interface region [1]. The chief drawback of LPE-grown films is an inferior surface morphology as compared to MOCVD or MBE methods.

But sometimes LPE-grown epilayers demonstrate relatively large areas with flat mirror-like surfaces. Understanding of their origin may help to improve morphology of LPE-grown layers. The purpose of this study was to investigate evolution of surface morphology of epitaxial layers at different steps of LPE growth run under conditions that give rise to such large flat areas in order to get insight into their microscopic formation mechanisms.

2. Experimental

LPE growth was carried out in a single-zone furnace with infrared heaters. Temperature was controlled by RIF-101 controllers to ±0.5 °C. Lattice-matched $Cd_{1-y}Zn_yTe$ ($y = 0.04 \pm 0.02$) wafers cut along <111> ± 0.5° from crystals grown by the vertical Bridgman method were used as substrates. The substrate parameters were as follows:

- optical transmittance within the $\lambda = (2.5..20)$ μm wave range, % 55 - 65
- specific resistance, Ohm·cm (T = 300 K) > 10^3
- dislocation density, N_D, cm^{-2} <10^5.

Prior to epitaxial growth, both sides of the substrates were subsequently chemomechanically and chemodynamically polished using bromine-alcohol solution.

Epitaxial layers, typically 10–40 μm thick, were grown from a Te-rich melt at temperatures in the range of 500–520°C on the <111>B side of the substrate.

To trace evolution of surface relief during the epilayer formation, two incomplete growth runs were also carried out:

1. Interaction of the substrate surface with the vapor phase above the melt, that involved heating up to the melting point of the growth solution, melt homogenization (τ = 30 min), and removing the melt without contact with the substrate.
2. The same as above, but the growth solution and the substrate were allowed to be in contact for a short time (τ = 3–5 min) before the melt removal.

The resulting surface morphology of the wafers was then examined *ex-situ* with the Nanoscope D3000 (Digital Instruments) atomic force microscope (AFM).

Composition of surface layers was analyzed with the X-ray fluorescence spectrometer SPRUT-2 of proprietary design of the Institute of Semiconductor Physics and Ukrrentgen (Ukraine).

3. Results and discussion

Typical features characteristic of surfaces of LPE-grown $Hg_{1-x}Cd_xTe$ epitaxial layers are irregularly shaped wandering in plan macroscopic terraces and plateau-like hillocks with flat tops. The hillocks are usually of the order of tens microns in lateral dimensions and located predominantly inside the hemiloops formed by the terraces. Another type defects are nearly hemispherical depressions of several micrometers in diameter frequently observed on flat tops of the hillocks. Surface morphology exhibiting peculiarities of that types was reported by many authors for LPE-grown layers of $Hg_{1-x}Cd_xTe$ [2–5] and also for many other materials [6]. But under certain growth conditions these plateau-like hillocks may become unusually large, up to few millimeters in diameter, and perfectly flat. This suggests that, in principle, morphology of the LPE-grown layers can be radically improved if the whole epilayer is grown as a single hillock. The following experimental results are related to evolution of surface morphology that finally leads to formation of such large hillocks.

Substrate morphology after melt homogenization step

Holding the substrate inside the growth ampoule at the melt homogenization temperature for 30 min. without contact with the melt resulted in visually observable surface roughening. Roughness was noticeably nonuniform across the surface, some areas looking more light than others. The resulting surface morphology is shown in Fig. 1, a - e. Evident traces of scratches can clearly be seen in the optical microscope image (Fig. 1a) thus suggesting that formation of surface morphology at this step is sensitive to surface pretreatment. The surface relief represents a relatively flat irregular pattern separated by clear-cut depressions (Fig. 1b, c). The further discussion depends on whether this relief results from the etching the substrate due to evaporation at the homogenization temperature or from the vapor phase $Hg_{1-x}Cd_xTe$ growth. A simple thermodynamic consideration can help to distinguish between these two possibilities. Composition of the growth solution used in this experiment was adjusted so that the growing epilayer is the $Hg_{1-x}Cd_xTe$ compound with $x \approx 0.2$, treated below as a quasibinary system $(HgTe)_{1-u}(CdTe)_u$. This means that the growth solution is in equilibrium at the growth temperature with the solid phase $u \approx 0.2$[7]:

$$\mu^l_{Hg} + \mu^l_{Te} = \mu^s_{HgTe} = G^{\circ s}_{HgTe} + RT \ln a^s_{HgTe} \quad (1a)$$

$$(\mu^l_{Hg} - \mu^{\circ l}_{Hg}) + (\mu^l_{Te} - \mu^{\circ l}_{Te}) = \mu^s_{HgTe} = \\ = \Delta G^\circ_f [HgTe(s)] + RT \ln(1-u)\gamma^s_{HgTe} \quad (1b)$$

where μ_A is a chemical potential of the A-component in the

Table 1. Comparison of CdHgTe epitaxy techniques

Growth technique	Advantages	Disadvantages
LPE	High purity, $(2\text{-}20)\cdot10^{14}cm^{-3}$ High growth rate Production scale-up	Inferior surface morfology and interface sharpness (2–3 μm) Multiple layers difficult Melt retention problems (when using Te-rich melts)
MOCVD	Good surface morfology Sharp interfaces (≤ 1 mm) Production scale-up	Purity of starting materials Marginal electrical properties
MBE	Composite structures, Sharpest interfaces, Superlattices Low growth temperature Good surface morphology In-situ analysis	Equipment expensive Low growth rate Stringent substrate surface preparation required Inferior electrical properties

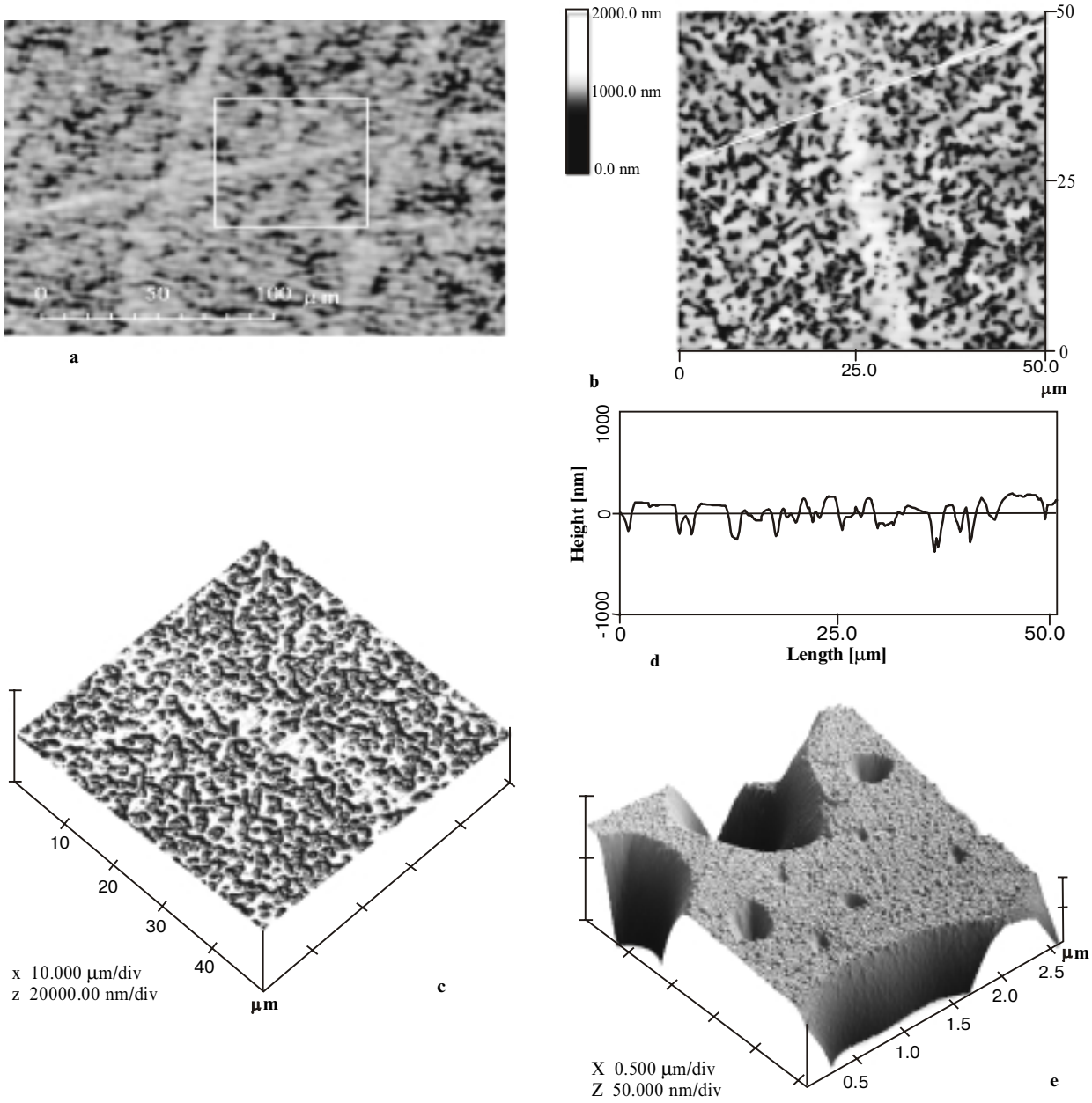

Fig.1. Surface morphology of $Cd_{0.96}Zn_{0.04}Te$ substrate after having been held inside the growth ampule at the melt homogenization temperature for 30 min without contact with the melt:
a – optical microscope image, b – AFM image, top view, c – AFM image, 3D view, d – crossection view, e – detailed image of surface pattern (part of a flat hillock top and an adjacent slope).

liquid or solid phase (superscripts *l* and *s*, respectively), G° is the standard Gibbs energy, and γ_A is the activity coefficient. Expressions for the Gibbs energies of HgTe and CdTe formation from the melt [8],

$$\Delta G_f^{\circ s}[HgTe(s)](cal) = -12829 + 8.339T - \\ - 4.0403(10^8)\times(-1.793/T + 251/T^2 + \\ + 0.001071)e^{-7135.68/T} \qquad (2a)$$

$$\Delta G_f^\circ[CdTe(s)](cal) = -30024 + 10.346T\ , \qquad (2b)$$

give (- 6.4) and (- 22.0) kcal/mol at $T = 773$ K, respectively. Taking into account these values, one can conclude from Eqs (1a, b) that difference in chemical potentials of Hg and Cd in the melt and the substrate will cause the mass transport to be directed from the melt to the substrate. Effect of mass transport from Hg-rich to Cd-rich compound of (Cd,Hg)Te system has been proved in experiments with isothermal vapor phase epitaxy [9,10]. Surface crossection pro-

file (Fig.1c) shows that the flat plateaus observable in the Fig.1b are different in height, that is more likely if the surface relief originates from the vapor phase $Hg_{1-x}Cd_xTe$ growth then from the evaporation etching. Direct confirmation of this conclusion is provided by the X-ray fluorescence analysis. Spectrum taken from the $Cd_yZn_{1-y}Te$ substrate (Fig.2) clearly demonstrates that the melt homogenization step gives rise to the Hg L_{a1} (1.24113 Å) spectral line.

These data show that the initially smooth <111>B oriented substrate become covered with the rough Hg-containing film during the melt homogenization step and the following LPE growth in fact proceeds upon a randomly oriented surface.

Epilayer surface after short-time growth step

After the substrate has been allowed to contact the growth solution for a short time (τ=3–5 min) the surface morphology was found to become typical for the LPE-grown layers (Fig. 3a) The plateaus atop hillocks were larger in size if compared with those after the melt homogenization step and partially merged (Fig. 3b). It should be noted that growth of hillocks proceeded nonuniformly across the layer. Surface image shown in Fig. 3b represents neighboring areas with different hillock sizes. It suggests that layer growth still remains sensitive either to substrate pretreatment or to surface morphology formed at the previous step. The X-ray fluorescence spectrum (Fig. 2) shows enhancement in the Hg L_{a1} line intensity.

Epilayer with large-size hillocks

Epitaxial $Hg_{1-x}Cd_xTe$ layers with perfectly flat hillocks up to several square millimeters in size were selected for further investigations. A considerable quantity of nearly circular depressions varying from ~50 to 500 nm in diameter was also observed (Fig. 4a). Nanoscale morphological investigation of plateaus atop hillocks using AFM revealed monomolecular growth steps and spirals originating from screw dislocations suggesting a dislocation-controlled facet growth mechanism (Fig.4b-d). Direct measurement of the step height (Fig.4b′) confirms their monomolecular nature. Monocrystalline $Cd_xHg_{1-x}Te$ has a zinc blend crystallographic structure with the lattice distance a = 0.646414 nm for x = 0.2. The zinc blend unit cell contains three monomolecular layers AII-BVI along the [111] directions. Therefore a single monomolecular layer of $Cd_xHg_{1-x}Te$ should be 0.373 nm thick, that is in excellent agreement with the experimentally observed value. Dislocations with larger Burgers vector component perpendicular to the surface possibly give rise to double-threaded spirals.

It should be noted that no growth steps were observed on the hillock tops after previous growth steps.

The plateaus are surrounded by steeply descending slopes without any specific morphological features except terraces flat at atomic scale and emerging from the defect sites (Fig. 4f). The letter is a clear indication that the growth proceeds not only at the plateaus, but at the slopes, too, the defect sites playing the role of obstacles for advancement of the slope. One can see that the boundary between the plateau and the slope is sharp at a microscopic scale. The fact that the microscopic growth mechanisms at the plateau and at the slopes are different possibly provokes inhomogeneous layer composition, known as a striation effect [6]. This effect results from different kinetics of incor-

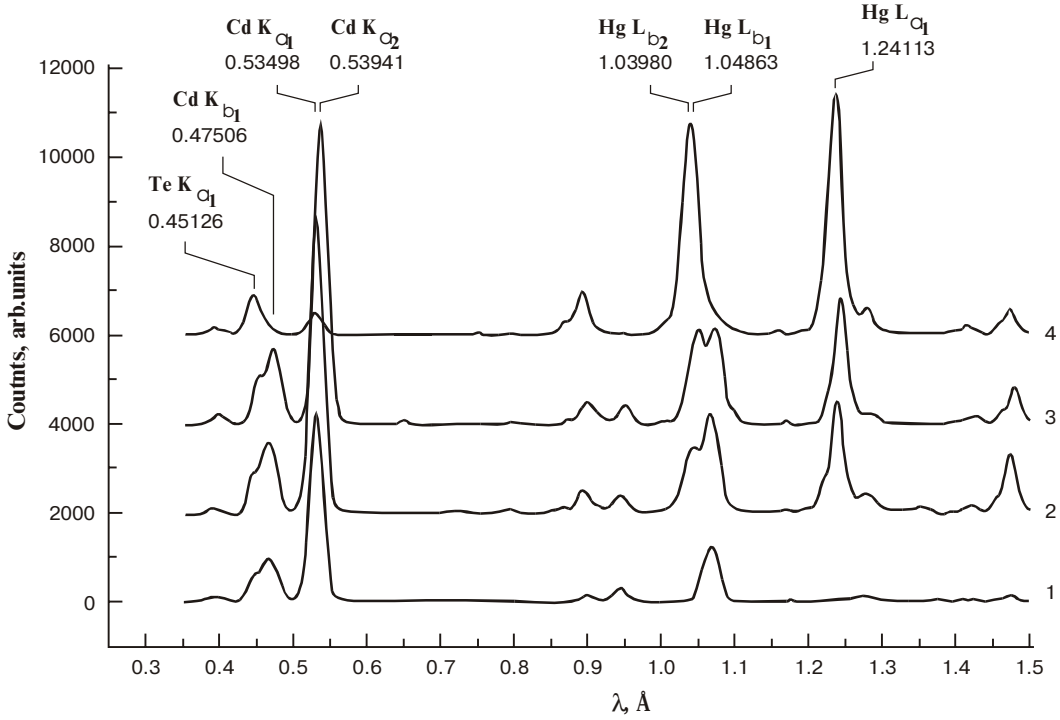

Fig. 2. X-ray luminescence spectra of surface layers on the $Cd_{0.96}Zn_{0.04}Te$ substrate after different steps of $Hg_{1-x}Cd_xTe$ epitaxial growth compared with bulk CdTe and HgTe etalons:
1 – bulk CdTe, 2 – after the homogenization step without contact with the melt, 3 – after a short-time LPE growth run, 4 – bulk HgTe.

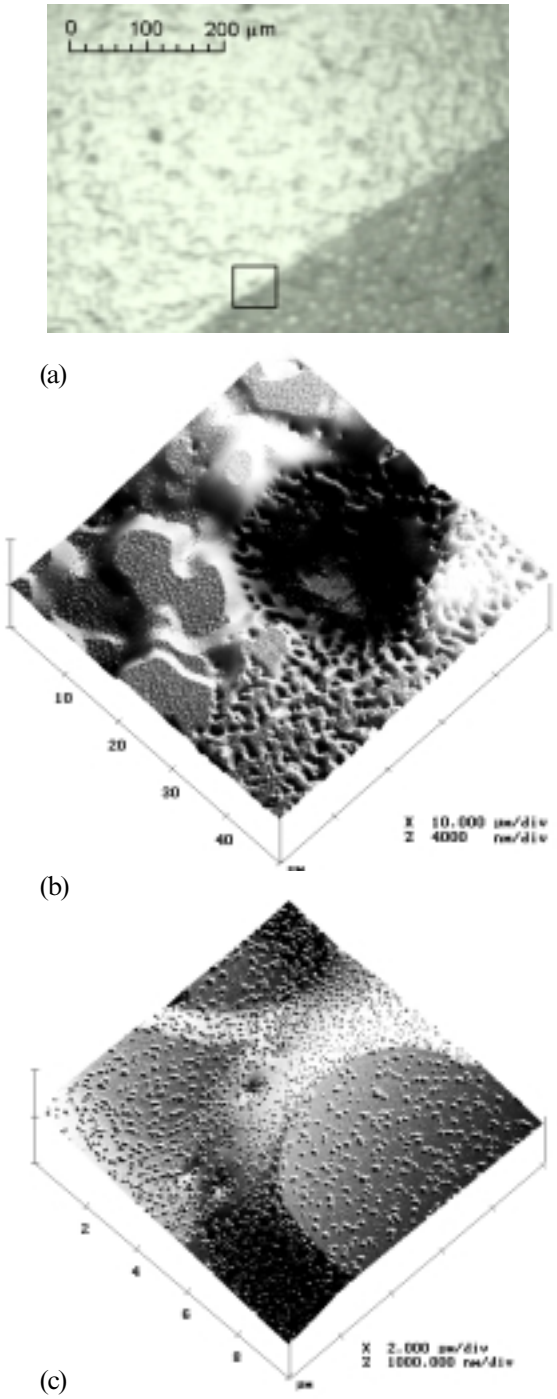

Fig.3. Surface morphology of $Hg_{1-x}Cd_xTe$ films after a short time (τ = 3-5 min) growth run. a – optical microscope image, b – AFM image, 3D view, c – detailed image of surface pattern

poration of species that form the crystal.

In principle, cause of the hillock formation may be different. Slopes surrounding hillocks may be considered as macrosteps resulting from merging the monomolecular steps. Macrosteps are known to be typical features of a majority of crystal faces and usually can be observed both on natural minerals and on laboratory grown crystals. The most apparent cases are the macrosteps risers of which are simple crystallographic planes growing layer-wise and sometimes suggestive of the faces of individual subcrys-tals. Such macrosteps grow at rates close to the rates of the major faces. Evidently, this mechanism is not involved in formation of the surface relief considered here. Macrosteps of frequent occurrence on perfect epilayers grown under well-controlled and sufficiently pure conditions typically are just bunches of elementary steps. Macrosteps of this type can be usually observed on facets of monocrystals and epitaxial films of elementary and multycomponent materials grown both from the melt and the gaseous phase using variety of growth techniques (VPE, CVD, MBE, etc.). The step bunches and the macrosteps terminated by stable crystallographic facets are well known to induce striations and inclusions [6]. Therefore, mechanisms of microstep bunching received considerable study promoted also by development of nanoscale visualization techniques. Nevertheless, current state of understanding fundamentals of this phenomenon unable to propose a rational way to control and exclude the appearance of step bunches.

It is generally accepted that nonlinearities of growth kinetics are the fundamental cause of step bunching [11]. Most elaborated microscopic models deal with crystal growth from vapor phase, where the interface kinetics only is of importance while bulk transport may be ignored. In these models, nonlinearities may appear due to various effects, from adsorption of impurities on the growing surface [6,11] to peculiarities of monomolecular step structure [12]. But recent studies of nucleation during vapor phase growth using *in situ* scanning tunneling microscopy revealed that the reality is even more complicated and correct models should account for effects of surface reconstruction too [13].

In the case of melt growth, both interface kinetics and bulk transport are essential, that makes theoretical consideration extremely sophisticated. Apart from mass and heat transport in the liquid phase, detailed knowledge of melt structure in terms of association ratio of dissolved species may be of importance. Results of elementary steps height measurement discussed above (Fig.4b′) show that the complete II-VI monomolecular layers only were present at the growth surface. It may suggest that the species that are in the associated form predominantly incorporate into growth sites. It seems also reasonable that kinetics of incorporation is different for associated and dissociated species. If so, the dissociated species adsorbed on the surface may even play a role of stoppers that hinder step advancement and thus influence the morphological stability of the interface growing from a binary solution and melt.

If the kinetic coefficients depend on supersaturation, an additional mechanism affecting the interface stability may become of importance. Its physical basis may be interpreted as follows. If the kinetic coefficient increases with supersaturation, then a protuberance on the interface sees a higher supersaturation and will grow faster than a depression, which sees a lower supersaturation, and hence there is enhanced instability.

To gain more insight into the step bunching mechanisms, experimental evaluation of the local supersaturation

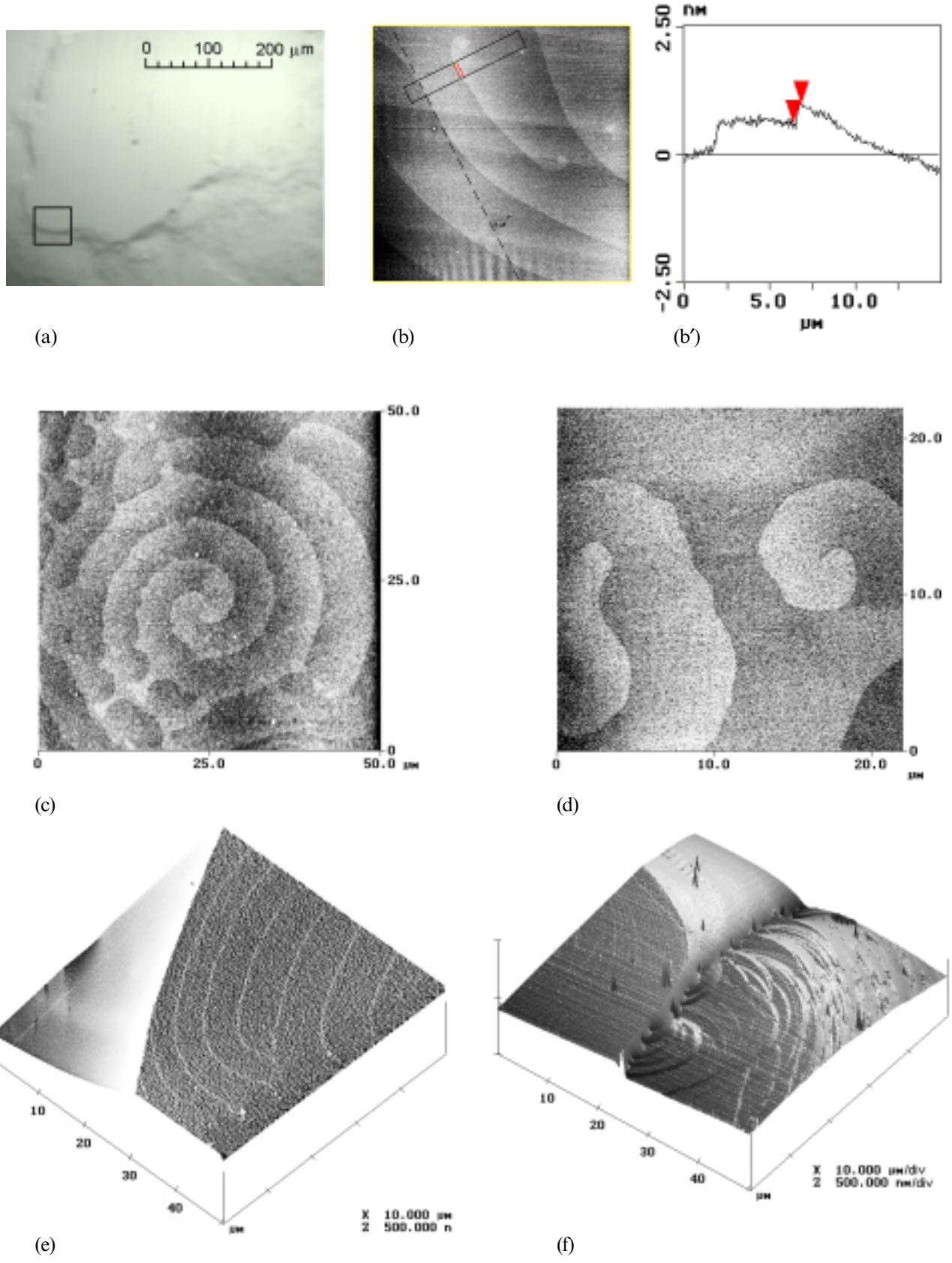

(a) (b) (b′)

(c) (d)

(e) (f)

Fig.4. Surface morphology of $Hg_{1-x}Cd_xTe$ epilayer with large-size hillocks after a full-time LPE growth run. a – optical microscope image, b,b' – crossection of the monomolecular step,c,d – AFM image of the hillock plateau (top view), e,f – AFM image of the hillock edge, 3D view.

in the vicinity of the growing surface would be advisable. In general, it is a complicated problem because it is difficult to gain access to this surface in the melt. A possible solution of this problem may come from analysis of a distance between the elementary steps originating from a single screw dislocation. For one-component systems, the driving force of growth from solution is the relative supersaturation $\sigma = (c - c_e)/c_e$, where c and c_e are the actual and equilibrium concentration of the solution. As has been shown by Cabrera and Levine [14], the effective supersaturation conditions at the surface can be estimated by measuring the distance between the monomolecular growth steps originating from the single screw dislocation. They gave the following relationship between the supersaturation and the interstep distance:

$$y_0 = 19r^* = \frac{19\gamma_m a}{kT\sigma}, \quad (3)$$

where r^* denotes the radius of the critical 2D nucleus at a given supersaturation, γ_m, a, k, T are step free energy per growth unit (or molecule), lattice distance, Boltzmann constant and growth temperature, respectively. The step free energy can be estimated as the energy per molecule on the edge of the critical nucleus, that is of the order of 1/6 of the heat of solution per molecule [15] that is ≈ 44 KJ·mol^{-1} for CdTe [16] Assuming a = 0.646414 nm, T = = 773 K and $y_0 \approx 10$ μm, expression (3) gives supersaturation value $\sigma = 8 \cdot 10^{-3}$. Unfortunately, this approach cannot be applied directly to the multicomponent crystals because of more complicated equilibrium conditions (see Eqs (1a,b)). Nevertheless, it can be considered as a phenomenological approximation until a more elaborated theory is developed.

Comparison of hillock sizes at different steps of epilayer formation suggests that they form from initial flat areas present at the surface after homogenization of the melt, the growth mechanisms being different at the plateaus and the surrounding slopes. The hillock size depends on difference between the vertical growth rate by dislocation-controlled mechanism and the velocity of lateral advancement of surrounding terraces.

Conclusions

AFM is an extremely valuable method for the *ex-situ* investigation of surface micromorphology of LPE-grown epitaxial layers providing insight into the microscopic growth mechanisms. It enables acquisition of high quality images of growth step patterns including monomolecular growth steps.

Epitaxial layers with unusually large flat areas were grown. It has been demonstrated that formation of these areas proceeded via a dislocation-controlled monomolecular step growth mechanism. No evidence of macrostep formation was observed across these areas. Surface composition analysis with X-ray fluorescence spectroscopy showed that vapor phase growth at the melt homogenization step contributed to epilayer formation and further evolution of its morphology. Phenomenological estimation of local supersaturation conditions giving rise to flat areas was given on the basis of the interstep distance of the growth spirals originating from screw dislocations. The results obtained suggest the way of radical morphological improvement of the LPE-grown epilayers.

Acknowledgements

Authors would like to thank Dr. S.Kavertsev for helpful discussions and suggestions during the course of this work and to Dr. P.Lytvyn for measurements and interpretation of X-ray fluorescence spectra.

References

1. H.Takigava, M.Yoshikawa, T.Maekawa, Dislocations in HgCdTe-CdTe and HgCdTe-CdZnTe heterojunctions// *Journal of Crystal Growth* **86**, pp. 446-451 (1988).
2. S.C.Gupta, «Key issues in substrate and liquid phase epitaxy of $Hg_{1-x}Cd_xTe$ from Hg-rich and Te-rich solutions», in *Fourth Inernational Conference on Material Science and Material Properties for Infrared Optoelectronics,* Fiodor F.Sizov, Editor,Proceedings of SPIE Vol. 3890,pp. 428-435 (1999).
3. Biao Li, Xiaoping Zhang, Jiqian Zhu, Junhao Chu, Crystallinity improvement of $Hg_{1-x}Cd_xTe$ fims grown by a liquid-phase epitaxial technique// *Journal of Crystal Growth* **184/185**, pp. 1242-1246 (1998).
4. C.A.Castro, J.H.Tregilgas, Recent developments in HgCdTe and HgZnTe growth from Te solutions// *Journal of Crystal Growth* **86**, pp. 138-145 (1988).
5. S.G.Parker, D.F.Weirauch, D.Chandra, Terracing in HgCdTe LPE films grown from Te solution// *Journal of Crystal Growth* **86**, pp. 173-182 (1988).
6. E.Bauser,H.P.Strunk, Microscopic growth mechanisms of semiconductors: experiments and models// *Journal of Crystal Growth* **69**, pp. 561-580(1984).
7. R.F.Brebrick, The thermodynamic modeling of the Hg-Cd-Te and Hg-Zn-Te systems// *Journal of Crystal Growth* **86**, pp. 39-48 (1988).
8. Tse Tung, Ching-Hua Su, Pok-Kai Liao, R.F.Brebrick, Measurements and analysis of the phase diagram and thermodynamic properties in the Hg-Cd-Te system// *J.Vac.Sci.Technol.* **21**(1), pp. 117-124 (1982).
9. J.C.Fleming, D.A.Stevenson, Control of the surface composition of isothermal vapor phase epitaxial mercury cadmium telluride// *J.Vac.Sci.Technol.* **A5**(6), pp. 3383-3385 (1987).
10. S.B.Lee, D.Kim, D.A.Stevenson, Growth and carrier concentration control of $Hg_{1-x}Cd_xTe$ heterostructures using isothermal vapor phase epitaxy and vapor phase epitaxy techniques// *J.Vac.Sci.Technol.* **B9**(3), pp. 1639-1645 (1991).
11. Coriell, A.A. Chernov, B.T. Murray, G.B. McFadden, Step bunching: generalized kinetics// *Journal of Crystal Growth* **183**, pp. 669-682 (1998).
12. Balykov, M. Kitamura, I.L.Maksimov, K.Nishioka, Growth and dissolution kinetics of step structure// *Journal of Crystal Growth* **198/199**, pp. 32-37 (1999).
13. Swartzentruber, Fundamentals of surface step and island formation mechanisms// *Journal of Crystal Growth* **188**, p.p. 1-10 (1998).
14. N.Cabrera, M.M.Levine, On the dislocation theory of evaporation of crystals// *Phil. Mag.* **1**, pp. 450-458 (1956).
15. C.Klementz, Hollow cores and step bunching effect on (oo1)YBCO surfaces grown by liquid-phase epitaxy// *J.Cryst.Growth* **187**, pp. 221-227 (1998).
16. N.N.Berchenko, V.E.Krevs, V.G.Sredin, *Semiconductor solid solutions and their applications*, Voenizdat, Moskov, 1982 (in Russian).